HHS Public Access

Author manuscript

Science. Author manuscript; available in PMC 2022 July 27.

Published in final edited form as:

Science. 2022 July 15; 377(6603): 276–284. doi:10.1126/science.abj8695.

TCR-Vγδ usage distinguishes pro-tumor from anti-tumor intestinal γδ T cell subsets

Bernardo S. Reis[1,†], **Patrick W. Darcy**[1], **Iasha Z. Khan**[1], **Christine S. Moon**[2], **Adam E. Kornberg**[2], **Vanessa S. Schneider**[1,3], **Yelina Alvarez**[1], **Olawale Eleso**[1], **Caixia Zhu**[1,4], **Marina Schernthanner**[1], **Ainsley Lockhart**[1], **Aubrey Reed**[1], **Juliana Bortolatto**[1], **Tiago B. R. Castro**[1], **Angelina M. Bilate**[1], **Sergei Grivennikov**[5], **Arnold S. Han**[2], **Daniel Mucida**[1,6,†]

[1]Laboratory of Mucosal Immunology, The Rockefeller University, New York, NY, 10065, USA.

[2]Department of Medicine, Division of Digestive and Liver Diseases, Columbia University, New York, NY, 10032, USA.

[3]Department of Biochemistry and Molecular Biology, Federal University of Parana, Curitiba, PR, Brazil

[4]Current address: Key Laboratory of Medical Molecular Virology, School of Basic Medical Sciences, Shanghai Medical College, Fudan University, Shanghai, 200032 China.

[5]Department of Medicine and Department of Biomedical Sciences, Cedars-Sinai Cancer Institute, Cedars-Sinai Medical Center, Los Angeles, CA, 90048, USA.

[6]Howard Hughes Medical Institute, The Rockefeller University, New York, NY, 10065, USA.

Abstract

[†]Correspondence: breis@rockefeller.edu (B.S.R.), mucida@rockefeller.edu (D.M.).

Author Contributions:
Conceptualization: BSR, DM
Data curation: TBRC, BSR, PWD, AMB
Formal Analysis: BSR, PWD, TBRC, AMB
Funding acquisition: DM, BSR, SG
Investigation: BSR, PWD, AL, AMB, CSM, AEK, ASH, IZK, VS, OE, CZ, AR, JB, MS
Methodology: BSR, SG, DM, AMB, JB
Project administration: BSR, DM
Resources: ASH, YA
Software: TBRC
Supervision: DM, BSR, SG
Validation: BSR
Visualization: BSR, TBRC
Writing – original draft: BSR, DM
Writing – review & editing: BSR, DM

Competing interests: The authors declare no competing financial interests.

Data and materials availability: E8I^{cre} mice were generated by Dan Littman (NYU) and obtained under a material transfer agreement (n. RU 2851) with the La Jolla Institute for Allergy & Immunology in 2013, and are available from The Jackson Laboratory (008766). *Scl2a1*$^{fl/fl}$ were generated and provided by Dale Abel under a material transfer agreement with The University of Iowa Research Foundation (n.2016-0268 / RU 17-011) in 2016, and available from The Jackson Laboratory (031871). Single-cell and bulk RNA-seq data were deposited in the Gene Expression Omnibus under accession number GSE205720.

γδ T cells represent a substantial fraction of intestinal lymphocytes at homeostasis, but also constitute a major lymphocyte population infiltrating colorectal cancers (CRC), albeit their temporal contribution to CRC development or progression remains unclear. Using human CRC samples and murine CRC models, we found that most γδ T cells in pre-malignant or non-tumor colons exhibit cytotoxic markers while tumor-infiltrating γδ T cells express a pro-tumorigenic profile. These contrasting T cell profiles were associated with distinct TCR-Vγδ gene-usage in both humans and mice. Longitudinal intersectional genetics and antibody-dependent strategies targeting murine γδ T cells enriched in the epithelium at steady state led to heightened tumor development, while targeting γδ subsets that accumulate during CRC resulted in reduced tumor growth. Our results uncover temporal pro- and anti-tumor roles for γδ T cell subsets.

One Sentence Summary:

Steady state γδ T cells prevent CRC development while infiltrating Vγ4$^+$ and Vγ6$^+$ RORγt-expressing γδ T cells promote tumor progression.

Intestinal intraepithelial lymphocytes (IELs) comprise a large T cell population located at the critical interface between the core of the body and the intestinal lumen, which is constantly exposed to food, commensal microbes, and pathogens. Previous observations have suggested an important role for IELs as a first line of immunity against pathogens (1-4). Among the main IEL subsets in mice or humans are T cells harboring the γδ T cell receptor (TCR). These γδ IELs are finely tuned to local epithelial signals and perform epithelial surveillance which is modulated through crosstalk with the intestinal epithelium (3, 5). In addition to their role in immune surveillance against enteric infections, γδ T cells have been associated to anti-tumor activity, including in human colorectal cancer (CRC) (6-11). CRC is currently the second most deadly cancer in the United States (ACS Inc., 2020). The cumulative risk of IBD patients developing CRC can reach 20%, however most CRC cases develop in patients without underlying inflammation. In both scenarios, tumor-elicited inflammation triggered by epithelial disturbances and microbial invasion is essential for survival of malignant cells and tumor growth (12-15). Here, we addressed whether epithelial resident γδ T cell subsets could prevent CRC development and whether phenotypically and functionally distinct γδ T cell subsets play a contrasting role, accelerating tumor progression.

Distinct profiles of infiltrating γδ T cells in both human and murine CRC

IL-17 producing γδ T cells preferentially utilize oxidative-phosphorylation metabolism and have been associated with increased tumor burden and poor survival in human cancers (16-18). In contrast, glycolytic IFN-γ–producing γδ T cells have been associated with protection against tumors and a better prognosis (19, 20). To characterize the gene signature of γδ T cells found in the intestine of CRC patients, we sorted γδ T cells from surgically dissected tumors and adjacent non-tumor areas, stimulated in vitro and performed single cell RNA sequencing (scRNAseq) utilizing the 10X genomics platform. We collected 1825 tumor-infiltrating and adjacent cells from 5 patients displaying at least 100 viable γδ T cells per region (out of 7 patients screened) (table S1 and fig. S1A and S1B). Pooled analysis of 716 cells from tumors and 1109 from non-tumor areas revealed 10 different

clusters (Fig. 1A). Tumor-infiltrating γδ T cells showed an overall increased cytokine signature (GO:0005126), including IL-17-producing γδ T cell-related genes, such as CD9 and LGALS3 (21) enriched in clusters 2 and 5, when compared to cells isolated from adjacent non-tumor areas (Fig. 1B and 1C). In contrast, γδ T cells isolated from adjacent non-tumor areas presented a cytotoxic-related profile, including the expression of GZMB and CXCR3, enriched in clusters 0 and 1, as well as the glycolysis-associated gene ENO1 and ALDOA (Fig. 1B and 1C, fig. 1SB and 1SC), an overall profile resembling IFNγ-producing γδ T cells (8). Clonal analysis of γδ T cells indicated clonal expansion in both non-tumor and tumor areas, with an enrichment for Vδ1 gene usage by tumor-infiltrating γδ T cells, while cells isolated from both areas displayed preference for Vγ4 (Fig. 1D and 1E, fig. 1SD to F). Additionally, we found a correlation between gene signature clusters and clonal expansion, confirming that expanded γδ T cell clones from tumors are enriched for IL-17-producing γδ T cell-related signature (cluster 2 and 5) while expanded clones in adjacent areas were enriched for IFNγ-producing γδ T cell signature (cluster 0 and 1) (Fig. 1E). Moreover, expanded clones related to the major gene expression clusters found in non-tumor areas (TRVG4_TRDV1 bias in cluster 1 and TRGV8_TRDV3 in cluster 0) were reduced in tumor sites, while clones related to the major gene expression clusters found in tumor areas (TRVG4_TRDV1 bias in cluster 2 and 5 and TRVG9_TRDV1 in cluster 3) were reduced in non-tumor areas (Fig. 1E). The above analyses indicate that γδ T cells enriched in human CRC areas share similarities to pro-tumorigenic IL-17-producing γδ T cells while cells found in tumor-adjacent areas display a CTL or IFNγ-producing γδ T cell signature, overall related to anti-tumor function.

To functionally and mechanistically assess the role of γδ T cells in CRC, we then employed two distinct CRC-mouse models: the chemical AOM-DSS colitis-associated CRC (CAC) (22) and the genetically inducible APC deficiency (14, 23, 24) (fig. S2A). Our initial characterization of γδ T cells in naïve animals confirmed a dominance by Vγ1 and Vγ7-expressing subsets, followed by $V\gamma4^+$ and $V\gamma6^+$ subsets at a low frequency (25-27), and changes in the expression of CD8αα homodimers according to proximal-distal and villus-crypt axes (fig. S2B to D). In colitis-associated CRC (AOM-DSS), we observed that tumor-infiltrating γδ T cells adopt both potentially anti- and pro-tumor phenotypes, with increased expression of CD107α and IFN-γ [associated with anti-tumor responses (13, 28)] as well as IL-17 [associated with pro-tumorigenic function (14, 28)](fig. S2E). $CD4^+$ $TCR\alpha\beta^+$ cells also display IFN-γ and IL-17–producing phenotypes, but in contrast to γδ T cells, expression levels upon restimulation are similar between tumor and non-tumor tissue sites (fig. S2F). In the CAC model, roughly 40% of IL-17–producing cells within the tumor are γδ T cells and about 30% are $CD4^+$ T cells (Th17 cells), while in non-tumor areas they correspond to roughly 35% and 20%, respectively (fig. S2G). Similar to what was observed in naïve mice, γδ T cells in healthy colon tissue display high expression of CD8αα, while a $CD8\alpha^-$ population expressing the exhaustion marker $PD\text{-}1^+$ is prominent among tumor–infiltrating γδ T cells (Fig. S2H and S2I). PD-1 expression segregated cells with potential anti-tumor ($PD\text{-}1^-$: IFN-γ^+) or pro-tumor phenotype ($PD\text{-}1^+$: IL-17^+ and IFN-γ^-) (Fig. S2J and S2K).

To gain information about γδ T cell dynamics during CRC progression, we longitudinally analyzed CRC mice harboring inducible APC floxed alleles, *Cdx2*$^{Cre\text{-}ER}$ x $APC^{fl/fl}$

(i*Cdx2*$^{\Delta APC}$). While virtually absent in naïve mice, we found that γδ T cells expressing IL-17 and PD-1 accumulate in the colonic tissue of i*Cdx2*$^{\Delta APC}$ mice upon tamoxifen injection, whereas the frequency of CD8α$^+$ γδ T cells decreases (Fig. 2A). Similar to our observations in the colitis-associated CRC model, the frequency of γδ T cells producing IFN-γ and IL-17 also increase among tumor-infiltrating lymphocytes (fig. S2L). Additionally, tumor infiltrating PD-1$^+$ (CD8α$^-$) preferentially express IL-17, while PD-1$^-$ (CD8α$^+$) preferentially secrete IFN-γ, with no overlap between IL-17 and IFN-γ producing γδ cells. (Fig. 2B to 2D and fig. S2M and S2N). CD4$^+$ T cells did not show significant differences in IL-17 and IFN-γ production between tumor or adjacent non-tumor areas (fig. S2O). In the APC loss model, about 60% of IL-17–producing cells within the tumor are γδ T cells, while Th17 cells constitute only 20% (fig. S2P). Outside tumor areas, almost 70% IL-17–producing cells are γδ T cells and roughly 10% are Th17 upon *in vitro* restimulation (fig. S2P). To further characterize tumor-infiltrating γδ T cells in the CAC model, we sorted these cells based on PD-1 expression and performed RNAseq analysis. Analogous to our observations in humans, murine CD8α$^+$PD-1$^-$ γδ T cells (blue) displayed increased expression of cytotoxic related genes (e.g. *Gzmb, Gzma, Lgals3, Lag3*), while CD8α$^-$PD-1$^+$ γδ T cells (red) showed increased expression of genes associated with IL-17 and pro-tumorigenic responses (15) such as *IL-17, Rorc* and *Il1r1* (Fig. 2E). These results suggest opposing phenotypes among γδ T cells found at steady state or in non-tumor areas, versus γδ T cells that accumulate during CRC in mice and humans.

Our bulk RNAseq analysis suggested divergent TCR usage between tumor-infiltrating CD8α$^-$PD-1$^+$ cells enriched in *TcrgV6* transcripts, and CD8α$^+$PD-1$^-$ γδ T cells, enriched in *TcrgV7* transcripts (Fig. 2E). To directly investigate the TCR repertoire of murine tumor–infiltrating γδ T cells, we single-cell sorted γδ T cells from the tumor and adjacent non-tumor areas of CRC mice subjected to either AOM-DSS or APC loss and performed single-cell TCR sequencing analysis (scTCRseq). In the APC loss model, γδ T cells from non-tumor areas are clonally diverse while tumor-infiltrating γδ T cells show noticeable clonal expansions (Fig. 2F). In the AOM-DSS model, we observed some clonal expansion within the Vγ7 subset found in non-tumor areas (Fig. 2F and fig. S2Q), an effect possibly related to the chronic inflammatory nature of this model (29), although most clonal expansions were also found in the tumor-areas (Fig. 2F). The expanded clones found in tumor areas in both models were primarily Vγ6$^+$Vδ1$^+$clones (*Trgv6* and *Trdv4* rearrangements), which are rarely observed in numbers in non-tumor areas or in the early phase of tumor development (Fig. 2F, G and fig. S2R). Flow cytometry analysis confirmed the relative increase of Vγ6$^+$ cells at the expense of decreased Vγ7$^+$ γδ T cells in the tumor areas (Fig. 2H and 2I). As suggested by the bulk RNAseq analysis, tumor-infiltrating Vγ7$^+$ and Vγ1$^+$ T cells isolated from mice subjected to AOM-DSS are mostly PD-1$^-$ and IFNγ$^+$, while Vγ6$^+$ cells express PD-1 and IL-17 (Fig. 2J). Overall, tumor-infiltrating PD-1$^+$ and IL-17$^+$ γδ T cells are composed of Vγ6 (56.5% ±5.2 and 71.2% ±7.5, respectively), while IFN-γ$^+$ γδ T cells are composed of Vγ1 (61.1% ±9.6) and Vγ7 (32.4% ±13.6) in the CAC model (Fig. 2J). Similar Vγ distribution was observed in tumor infiltrating TCRγδ$^+$ T cells isolated from CRC mice subjected to APC loss (fig. S2S). Immunofluorescence imaging of the colonic tissue from tamoxifen-treated i*Cdx2*$^{\Delta APC}$ mice confirmed the preferential accumulation of PD-1 expressing γδ T cells in tumor areas (fig. S2T). The analyses above suggest that

tumor infiltrating γδ T cells are composed of four major subsets based on Vγ-usage, divided into two functional groups: polyclonal murine Vγ7$^+$ and Vγ1$^+$ resembling human IFN-γ-producing γδ T cell subsets (enriched in cluster 0 and 1, see Fig. 1A), which exhibit an "anti-tumor" cytotoxic program, and clonally-expanded murine Vγ6$^+$Vδ1$^+$ that express PD-1 and secrete IL-17, which in turn resemble human IL-17-producing γδ T cell subsets (enriched in cluster 2 and 5, see Fig. 1A).

Anti-tumor activity by epithelium-resident murine Vγ1$^+$ and Vγ7$^+$ γδ T cells

To address whether the phenotype of epithelium-resident TCRγδ T cells plays a role in restricting CRC development, we first subjected *Trdc*$^{-/-}$ knockout mice, which are deficient in γδ T cells, to the AOM-DSS model (fig. S3D to F). Because *Trdc*$^{-/-}$ animals are more susceptible to the experimental DSS regimen (30), we used a lower DSS concentration (1%), which does not result in noticeable inflammation or tumor development in wild-type control mice (fig. S3E and fig. S3A to C). In line with previous literature (10), following the 1% DSS regimen, *Trdc*$^{-/-}$ mice displayed enhanced inflammation and significant increase in tumor development, again suggesting an anti-tumor, or anti-inflammatory role for intestinal epithelium-resident γδ T cell populations (fig. S3E and S3F). Because total *Trdc*-deficiency also prevents the accumulation of γδ cells during tumor progression, we next aimed to preferentially restrict epithelium-resident γδ T cell function by inducible hemizygous or homozygous inactivation of *Scl2a1* (i*Trdc*$^{Scl2a1fl/+}$ or i*Trdc*$^{\Delta Scl2a1}$) encoding the glucose transporter Glut1. We have previously reported that epithelium-resident γδ T cells control early invasion by *Salmonella* Typhimurium via a metabolic switch towards glycolysis that is dependent on Glut1 expression (3), an observation related to recent findings showing that IFN-γ−, but not IL-17–secreting γδ T cells, are glycolytic and exert anti-tumor activity (31). Our analysis of human samples described above also pointed to glycolytic γδ T cells that were preferentially found in the tumor-adjacent areas. We then subjected i*Trdc*$^{\Delta Scl2a1}$, i*Trdc*$^{Scl2a1fl/+}$, and littermate control mice to the AOM-DSS model (Fig. 3A). Early targeting of Glut1 in γδ T cells results in higher tumor number and load when compared to control animals, without affecting tumor size (Fig. 3B). Moreover, while Glut1 inactivation does not lead to changes in CD8α, PD-1 or IL-17 expression by γδ T cells, we detected a significant reduction in IFN-γ production by tumor-infiltrating γδ T cells in both i*Trdc*$^{Scl2a1fl/+}$ and i*Trdc*$^{\Delta Scl2a1}$ mice when compared to littermate controls (Fig. 3C and 3D and fig. S3G). We did not observe a reduction in tumor–infiltrating γδ/αβ cell ratio or in the frequency of Vγ7$^+$ cells in tamoxifen-treated i*Trdc*$^{Scl2a1fl/+}$ mice (fig. S3H), overall reinforcing the notion that Glut1 does not play a major role on γδ T cell maintenance, but is required for epithelium-resident γδ T cell function (3). Inactivation of Glut1 in γδ T cells did not affect the frequency of IFN-γ production by TCRαβ$^+$CD8αβ$^+$ cells (fig. S3I). In contrast, late Glut1 targeting (after the second DSS cycle) had no impact on tumor load or tumor-infiltrating γδ T cells (fig. S3J to N). These results suggest that epithelium-resident γδ T cells exert immunosurveillance against epithelial tumors and early functional impairment of Glut1–dependent γδ T cells favors CRC development.

To directly access an anti-tumor role of epithelium-resident γδ T cells, we generated Vγ7$^{-/-}$ mice by CRISPR/Cas9 genome editing (fig. S4A to S4E). At steady-state, Vγ7$^{-/-}$ mice display no changes in the tissues analyzed besides the intestine, which show an overall

reduction of γδ T cells; a decrease was also observed, albeit in lesser degree, in Vγ7$^{+/-}$ mice, suggesting allelic exclusion by the unproductively-rearranged TCR (fig. S4B to E). TCRαβ^{+} T cells showed no differences in the organs analyzed, except for an increase in frequency of TCRαβ^{+}CD8αα^{+} "natural" IELs, suggesting a compensatory mechanism in the reduction of γδ IELs (fig. S4C). Vγ7$^{-/-}$ mice subjected to AOM-DSS treatment did not show differences in tumor number, size and burden when compared to Vγ7$^{+/-}$ or Vγ7$^{+/+}$ littermate controls (fig. S5A to S5G). Moreover, though there was a significant reduction in TCRγδ cells in non-tumor areas of Vγ7$^{-/-}$ mice (assessed by the ratio of TCRγδ^{+} to TCRαβ^{+}), the frequencies of IFN-γ, PD-1 and IL-17 expression by γδ T cells were similar between Vγ7$^{-/-}$ and Vγ7$^{+/-}$ littermate controls (fig. S5C to S5E). Finally, tumor-infiltrating TCRαβ^{+}CD4^{+} and TCRαβ^{+}CD8α^{+} cells did not show differences in cytokine production between Vγ7$^{-/-}$ mice and Vγ7$^{+/-}$ littermate controls (fig. S5G). To address a possible compensatory role of Vγ1^{+} γδ T cells in anti-tumor immunity in the absence of Vγ7^{+} cells, we administered α-Vγ1 depleting antibodies (clone 2.11), starting one week before AOM-DSS treatment until the second DSS treatment, to Vγ7$^{-/-}$, Vγ7$^{+/-}$ and littermate controls (Fig 3E to 3I). Both Vγ7$^{-/-}$ and Vγ7$^{+/-}$ mice treated with α-Vγ1 depleting antibodies showed increase tumor number and burden (Vγ7$^{+/-}$ group only) compared to treated littermate controls (Fig. 3E). Again, we observed a significant reduction in the ratio of TCRγδ^{+} to TCRαβ^{+} cells in the tumor for both Vγ7$^{+/-}$ and Vγ7$^{-/-}$ mice compared to littermate controls (Fig. 3F). In addition, we did not observe differences in tumor infiltrating Vγ subsets besides Vγ7^{+} cells, suggesting that antibody-mediated depletion of Vγ1 cell was restricted to early stages of tumor progression (Fig 3G). Nevertheless, we observed a reduced frequency of CD8αα-expressing γδ T cells in both tumor and non-tumor areas, and an increased frequency of PD-1^{+} cells in non-tumor areas in Vγ1-depleted Vγ7$^{-/-}$ mice compared to littermate controls (Fig. 3H and 3I). We did not observe differences in IFN-γ or IL-17 production by tumor-infiltrating γδ T cells (Fig. 3H and 3I). Additionally, tumor infiltrating TCRαβ^{+}CD4^{+} and TCRαβ^{+}CD8α^{+} cells did not show differences in cytokine production between the groups (fig. S5H). Together, these data suggest that murine epithelium-resident Vγ1^{+} and Vγ7^{+} intestinal γδ T cells are important in the early control of tumor formation.

Pro-tumor role of infiltrating murine Vγ4^{+} and Vγ6^{+} γδ T cells

While our observations point to an important anti-tumor function for epithelium–resident γδ T cells, previous studies have also described that the tumor microenvironment, or the microbiome, can influence γδ T cell subsets to have an opposite, pro-tumorigenic role during cancer progression (3). We therefore questioned whether the clonally expanded Vγ6^{+} PD-1^{+} IL-17 producing γδ T cells that accumulate among tumor infiltrating lymphocytes contribute to CRC progression. We conditionally deleted Rorγt, which is the main transcription factor linked to IL-17 production in T cells (32), using the same strategy described above. To specifically target γδ T cells that accumulate during CRC progression, we treated i*Trdc*$^{\Delta Rorc}$ and littermate control mice with tamoxifen after the second DSS cycle (fig. S6A to S6H). While no differences in tumor numbers or burden were noted, late Rorγt deletion in γδ T cells results in smaller tumors (fig. S6B). Accordingly, this strategy leads to altered Vγ-usage among tumor infiltrating γδ T cells: tamoxifen–

treated i*Trdc*$^{\Delta Rorc}$ mice display significantly decreased Vγ6$^+$ and Vγ4$^+$ populations when compared to littermate controls (fig. S6C). Tamoxifen-treated i*Trdc*$^{\Delta Rorc}$ mice do not display changes in CD8$\alpha\alpha$-expressing $\gamma\delta$ T cells (fig. S6D). However, late Rorγt targeting results in reduced frequency of PD-1$^+$ and IL-17–producing (71.2% and 39.08% suppression, respectively) tumor-infiltrating $\gamma\delta$ T cells, affecting both Vγ6$^+$ and Vγ4$^+$ populations (fig. S6C to S6E). Overall, we observed a 55% reduction in tumor infiltrating Rorγt$^+$ $\gamma\delta$ T cells in i*Trdc*$^{\Delta Rorc}$ after tamoxifen treatment when compared to littermate controls (fig. S6E). No difference was noted in Rorγt expression nor IL-17 production among CD4$^+$ T cells (fig. S6F). Tumor infiltrating CD8$\alpha\beta^+$ T cells displayed increased IFN-γ production in i*Trdc*$^{\Delta Rorc}$ mice, when compared to littermate controls (fig. S6G). IL-17, and additional pro-inflammatory cytokines, have been shown to promote tumor growth via recruitment of "monocytic myeloid-derived suppressor cells" (M-MDSCs), inflammatory monocytes (both gated as CD11b$^+$Gr-1^{int}) and neutrophils, or granulocytic MDSCs (G-MDSCs, both gated as CD11b$^+$Gr-1^{high}) (14, 16, 17, 19, 33-35). Accordingly, we observed a significant decrease in tumor-infiltrating CD11b$^+$Gr-1^{int} cells in i*Trdc*$^{\Delta Rorc}$ mice when compared to littermate controls (fig. S6H). These data indicate that Rorγt expression by $\gamma\delta$ T cells is an important factor for the accumulation of IL-17–producing Vγ4$^+$ and Vγ6$^+$ TCR$\gamma\delta^+$ cells, which in turn contribute to a pro-tumorigenic microenvironment.

Changes in resident bacterial communities have been associated to tumor burden in CRC models (14) and were shown to impact pro-tumorigenic T cells, including Rorγt$^+$ IL-17–producing Vγ6$^+$ $\gamma\delta$ T cells, in both lung and ovarian cancer models (33, 36). Due to complex changes in gut microbiota composition after cycles of DSS treatment (36), we focused on the impact of microbiota changes and antibiotic treatment in the APC loss model. 16S ribosomal RNA sequencing from feces of mice subjected to the APC loss model revealed a sharp decrease in microbial diversity as well as broad changes in bacterial composition that can be detected as early as 2 weeks after tamoxifen administration and continue in the following timepoints (fig. S7A and S7B). Consistent with a role of gut microbiota in promoting tumor growth (14), subjecting tamoxifen-treated i*Cdx2*ΔAPC mice to a broad-spectrum antibiotic cocktail (ABX; Ampicillin, Vancomycin, Metronidazole and Neomycin) for only one week results in smaller tumors while not impacting tumor number or burden, resembling changes observed upon late Rorγt targeting in the CAC model (Fig. 4A and 4B). CD8$\alpha\alpha^+$ $\gamma\delta$ T cells, primarily represented by Vγ1$^+$ and Vγ7$^+$ cells, display increased frequency in both non-tumor and tumor sites in mice receiving ABX treatment (Fig. 4C). Moreover, ABX treatment results in reduced frequency of IL-17– and PD-1–expressing $\gamma\delta$ T cells (both over 75% suppression), primarily within the Vγ6$^+$ subset (Fig. 4D and 4E), even though Vγ6$^-$ $\gamma\delta$ T cells (mostly comprised of Vγ4$^+$) also contribute to PD-1 and IL-17 expression in tumor sites (see fig. S2Q). To address whether Vγ6$^+$ cells accumulate during CRC progression due to increased recruitment or *in situ* proliferation, we performed *in vivo* EdU labelling. We observe higher proliferation rates in Vγ6$^+$ *versus* Vγ6$^-$ $\gamma\delta$ T cells, which are reduced (56.7%) upon ABX treatment (Fig. 4F and 4G). Although microbiota depletion in tamoxifen-treated i*Cdx2*$^{\Delta APC}$ mice led to a decrease in intra-tumoral Vγ6$^+$ $\gamma\delta$ T cells, it did not affect Vγ4$^+$ cells (Fig. 4H). Additionally, contrary to what was observed upon late Rorγt targeting in the CAC model, we did not observe changes in frequency of IFN-γ-producing CD8$\alpha\beta^+$ T cells or CD11b$^+$Gr-1$^+$ (both

high and intermediate) cells in tumor areas of ABX treated animals (fig. S7C and S7D). These observations point to distinct susceptibility following microbiota manipulations by two main subsets of tumor-accumulating γδ T cells. Specifically, Vγ6$^+$, but not Vγ4$^+$ cells, proliferate in response to microbiota and depend on microbiota signals to sustain PD-1 and IL-17 expression, as well as to boost tumor growth.

Because of their temporal dynamics and distinct functional properties were segregated based on TCR V-usage, we investigated a possible role for TCR engagement by epithelium-resident vs tumor-infiltrating γδ T cells. We treated i*Cdx2*$^{\Delta APC}$ with anti-TCRγδ blocking (non-depleting) antibodies (UC7-13D5) for two weeks starting seven days before tamoxifen administration, therefore targeting TCRγδ-mediated signaling primarily on epithelium-resident Vγ1$^+$ and Vγ7$^+$ cells (fig. S7E). Early TCRγδ blockade did not impact tumor number or size (fig. S7F), γδ/αβ ratio (fig. S7G), or frequencies of CD8α$^+$, PD-1$^+$ and IL-17 and IFN-γ -producing γδ T cells compared to control mice (fig. S7H and S7J). Additionally, while tumor-infiltrating PD-1$^+$ cells show higher proliferation rates compared to PD-1$^-$ counterparts, early anti-TCRγδ treatment did not affect proliferation rates (fig. S7I). TCRγδ blocking did not affect CD4$^+$ T cell proliferation (fig S7K).

Next, we treated i*Cdx2*$^{\Delta APC}$ with anti-TCRγδ blocking antibody for two weeks starting three weeks post initial tamoxifen treatment, hence also targeting TCRγδ-mediated signaling on tumor-infiltrating Vγ4$^+$ and Vγ6$^+$ cells (Fig. 4I). Late TCRγδ blockade led to a significant decrease in tumor size and burden but did not change tumor number (Fig. 4J). The γδ/αβ ratio, assessed by *Trdc*^{GFP}-driven GFP signals, was reduced in tumor areas while the frequency of CD8αα$^+$ γδ T cells both in tumor and adjacent areas was increased (Fig. 4K and 4L). Consistent with a preferential effect of late TCRγδ blockage on tumor-infiltrating Vγ4$^+$ and Vγ6$^+$ cells, we found a significant decrease in both PD-1$^+$ and IL-17 -producing γδ T cells in tumor areas (Fig 4L and 4M). TCR blockade did not lead to changes in the frequency of IFN-γ-producing CD8αβ$^+$ T cells or CD11b$^+$Gr-1$^+$ (both high and intermediate) cells (fig. S7L and S7M). *In vivo* EdU labeling confirmed that the heightened PD-1$^+$ γδ T cell proliferation rate in tumor areas is TCR dependent (Fig. 4N). Late TCRγδ blocking did not affect CD4$^+$ T cells proliferation (fig S7N).

TCR engagement is associated with T cell movement arrest (37). To investigate whether the apparent TCR-dependent proliferation and pro-tumorigenic function of tumor-infiltrating γδ T cell subsets correlate with cell motility changes, we performed live intravital multiphoton microscopy on cells from i*Cdx2*$^{\Delta APC}$ *Trdc*^{GFP} reporter mice immediately before, one and three weeks after tamoxifen treatment (Fig. 4O and 4P). Though we were unable to ascertain tumor borders or pre-tumor regions in the timepoints analyzed, total T cell displacement was overall consistent along timepoints, and between cecal and colonic areas. Compared to videos obtained in mice pre- or one-week post-tamoxifen treatment, colonic γδ T cells displayed reduced speed at three weeks post-tamoxifen, suggesting ongoing TCR engagement (Fig. 4P, Movie S1 and S2). Of note, this time point coincides with accumulation of Vγ6$^+$ cells in the colon of i*Cdx2*$^{\Delta APC}$ mice after tamoxifen treatment (see Fig. 2G). Consistent with this notion, TCR blockade with *in vivo* anti-TCRγδ antibody treatment rescued cell velocity to the levels observed before or early after APC loss (Fig. 4P and fig. S7O). These results suggest that epithelium-resident anti-tumor γδ T cell subsets

may function in a TCR-independent manner while the γδ T cell subsets that accumulate during tumor progression function to boost tumor growth via the TCR.

Our findings so far indicate that IL-17–producing, or PD-1–expressing tumor–infiltrating γδ T cells are composed ~70-85% of microbiota-dependent Vγ6$^+$, and ~10-20% of Vγ4$^+$ cells. To directly assess the roles of Vγ4$^+$ and Vγ6$^+$ γδ T cells in CRC progression, we generated Vγ4$^{-/-}$ and Vγ6$^{-/-}$ mice by CRISPR targeting of *Trgv4* and *Trgv6* genes, respectively (fig. S8A-E and fig. S9A-E). Fully backcrossed Vγ4$^{-/-}$ mice were subjected to AOM-DSS and show no differences in tumor number, tumor size or tumor-infiltrating γδ T cells (aside from Vγ4) when compared to heterozygous littermate controls (fig. S10A-G). The ratio of γδ/αβ T cells among of tumor-infiltrating lymphocytes in Vγ4$^{-/-}$ mice remain the same as the ratio observed in Vγ4$^{+/-}$ controls (fig. S10B), suggesting a compensatory expansion of remaining γδ T cells, including Vγ6$^+$ T cells, in the absence of Vγ4$^+$ subset.

We next analyzed B6-backcrossed naïve Vγ6$^{-/-}$ mice, which display a decreased γδ/αβ T cell ratio in the fat tissue at steady state, suggesting a lack of compensatory expansion of Vγ4$^+$ cells in non-inflammatory settings (fig. S9B). Like Vγ4$^{-/-}$ mice, Vγ6$^{-/-}$ mice subjected to AOM-DSS displayed similar CRC development, progression (Fig. 5A) and parameters of tumor-infiltrating γδ T cells to Vγ6$^{+/-}$ littermate controls (Fig. 5B to F). The absence of an otherwise large intra-tumor Vγ6$^+$ population did not result in altered γδ/αβ T cell ratio (Fig. 5B), explained by a compensatory increase in other γδ T cells, particularly Vγ4$^+$ cells in tumor settings (Fig. 5C). Indeed, in the absence of Vγ6$^+$ cells, we observed a sharp increase in tumor-infiltrating Vγ4$^+$ cells producing IL-17 (Fig. 5F). To address whether deletion of Vγ6 led to biased clonal expansion in the remaining cells, we performed scTCRseq in Vγ4$^+$ cells in Vγ6$^{-/-}$ mice subjected to AOM-DSS. We identified large clonal expansions in Vγ6$^{-/-}$ mice albeit similar to those observed in littermate control mice, both in tumor and non-tumor areas (fig S10H and S10I). We did not observe differences in tumor–infiltrating CD4$^+$ T cells between Vγ6$^{-/-}$ and Vγ6$^{+/-}$ mice (fig. S10J). The overall similar tumor development and composition of tumor-infiltrating γδ T cells in Vγ4$^{-/-}$ and Vγ6$^{-/-}$ mice raised the possibility that tumor-infiltrating, PD-1$^+$ IL-17–producing Vγ4$^+$ and Vγ6$^+$ populations play redundant roles in promoting CRC growth.

To address possible compensatory, and redundant, roles between tumor–infiltrating Vγ4$^+$ and Vγ6$^+$ γδ T cells, we treated Vγ6$^{-/-}$ and Vγ6$^{+/-}$ littermate control mice with depleting anti-Vγ4 antibody (UC3-10A6) starting after the second DSS cycle until analysis. In contrast to untreated Vγ6$^{-/-}$ mice, Vγ4–depleted Vγ6$^{-/-}$ mice developed significantly smaller tumors than Vγ4-depleted Vγ6$^{+/-}$ littermate control mice, while no significant changes in tumor numbers or load were noted (Fig. 5G). In contrast to previous strategies, Vγ4–depleted Vγ6$^{-/-}$ mice display a roughly 50% reduction in tumor infiltrating γδ/αβ T cell ratio (Fig. 5H). Vγ4–depleted Vγ6$^{-/-}$ mice also display enhanced intra-tumoral CD8αα$^+$ γδ T cells when compared to Vγ4-depleted Vγ6$^{+/-}$ mice (Fig. 5J), similar to what was observed in ABX-treated mice in the APC loss mouse model. Additionally, and consistent with a functional redundancy between Vγ4$^+$ and Vγ6$^+$ γδ T cells, Vγ4–depleted Vγ6$^{-/-}$ mice show about 80% reduction in the frequency of PD-1$^+$ and IL-17–producing γδ T cells within the tumor (Fig. 5J to L). We did not observe changes in cytokine production by CD4$^+$ or CD8αβ$^+$ T cells (fig. S10K and S10L) or in frequency of CD11b$^+$Gr-1^{int} cells;

however, Vγ4–depleted Vγ6$^{-/-}$ mice showed a significant decrease in CD11b^{+}Gr-1^{high} cells at tumor sites (fig. S10M), a phenotype likely also linked to the suppression of intra-tumoral IL-17 secretion by T cells. Hence, in sharp contrast to an anti-tumor role by epithelium-resident subsets, dominated by Vγ1^{+} and Vγ7^{+} γδ T cells, these data suggest redundant roles of tumor-infiltrating Vγ4^{+} and Vγ6^{+} γδ T cells in promoting CRC progression.

Discussion

Tumor–infiltrating lymphocytes are essential components of anti-tumor responses and represent major targets for immunotherapies (6, 11, 19, 38). The cytokine and metabolic profiles of γδ T cell subsets found in human and murine CRC implied opposing roles by γδ T cells found in the non-tumor or steady-state epithelium *versus* γδ T cells that accumulate during cancer progression. Gain- and loss-of-function studies in mouse models confirmed that epithelial surveillance by steady-state IFN-γ–producing cytotoxic γδ populations help prevent tumor initiation, while accumulating intra-tumor γδ T cells support tumor progression.

Specialized “dendritic epidermal T cells” (DETC) γδ T cells in the skin, mostly comprised of Vγ5^{+} cells have been shown to suppress tumor development via an NKG2D–dependent cytotoxic mechanism (2, 39, 40), while dermal γδ T cells, pre-committed to IL-17 production and expressing Vγ4 or Vγ6, were shown to promote tumor growth (19). While these observations parallel our findings, whether such anatomical segregation can also be observed in the intestinal epithelium *versus* lamina propria in specific conditions (27), remain to be determined. Our observations in the intestine indicate that γδ IELs in pre- or non-tumor areas harbor a diverse TCR repertoire while sharing primarily Vγ1 or 7 segments, particularly in the APC loss model. The accumulation of Vγ7^{+} IELs was previously linked to binding of the germline Vγ7 chain to Btnl proteins; a tissue-specific selection not associated with TCRγδ CDR3 region (27). Analogous to changes we observed in γδ T cells during CRC progression, previous studies described an irreversible expansion and repertoire reshaping of γδ T cells in chronically inflamed conditions such as in Celiac patients (40). Another important parallel with this study is their observation that γδ T cells from patients with active disease acquire a pro-inflammatory cytokine profile in contrast to γδ T cells isolated from patients in remission, which are primarily cytotoxic (40).

Our data collected on human specimens revealed expanded Vγ4Vδ1 and Vγ8Vδ3 “epithelial-resident” cells located in tumor-adjacent areas with strong cytotoxic gene signature, suggesting anti-tumor activity paralleling murine Vγ1/Vγ7. However, in contrast to a clear functional segregation of murine γδ T cells based on their Vγ-usage, intra-tumor Vγ4Vδ1 cells displayed gene signatures associated with an intratumor metabolic adaptation, and pro-tumorigenic function. In this line, a recent study on breast cancer proposed that tumor-infiltrating Vδ1^{+} cells may have an immunosuppressive function (41). It is possible that this discrepancy between human and mouse data could be result of their disparate timing of CRC progression. Indeed, a long-term exposure to the tumor microenvironment has been proposed to suppress an anti-tumor cytotoxic function by human gut-resident Vδ1^{+} clones (6). Additionally, metabolic disorders have been linked to a decrease in tissue-resident γδ T cells during early tumorigenesis (9). Supporting the possibility of

metabolic adaptation, a recent study uncovered a metabolism-driven dichotomy in γδ T cell function: IL-17-producing γδ T cells are found to be dependent on oxidative phosphorylation, thriving in lipid-rich environments such as tumors; IFN-γ–producing γδ T cells required glycolysis for their energy expenditure (31). Conversely, previous observations suggested a role for clonally–restricted IL-17–producing T cells, including γδ cells, in tumor-progression (14, 33, 36). These reports are in line with our observations that, like their response to invading bacteria (3), IFN-γ–producing γδ T cells, particularly $V\gamma1^+$ and $V\gamma7^+$ subset, display anti-tumor activity dependent on Glut1 expression, while IL-17–producing γδ T cells, particularly the Vγ6Vδ1 clone, were highly expanded in tumor areas.

Our study has several limitations. While our results and previous literature (14, 16, 17, 19, 33, 34), point to a tumor-progression role for intra-tumoral IL-17, which downstream mechanisms induced by IL-17, such as neutrophil and MDSCs recruitment, are necessary for regulation of tumor growth remain to be defined. Because IL-17 production by γδ T cells in the gut has also been linked to tissue repair (42), it remains possible that in addition to IL-17, additional factors or molecules expressed by $V\gamma4^+$ or $V\gamma6^+$ cells aid tumor growth in the balance with tissue repair mechanisms. It remains unclear whether high PD-1 expression, specific localization within the tumor, or other factors, distinguish a tumor progression role for γδ T cells *versus* other IL-17–secreting cells, such as Th17 cells. Additionally, our studies did not define the mechanisms by which the tumor microenvironment mediates the accumulation of microbiota–dependent $V\gamma6^+$ and microbiota–independent $V\gamma4^+$ subsets that aid tumor growth; it is tempting to speculate that analogous mechanisms to the Btnl–dependent Vγ7 selection (26, 27, 43, 44), are utilized. Indeed, a recent study suggests that expression of Btnl2 by tumor cells can specifically recruit pro-tumorigenic IL-17–producing γδ T cells (45). While the reduced number of patients, and cells, analyzed limit broader generalizations regarding public clones, TCR usage-biases and linked signatures, our analyses of infiltrating γδ T cells in human CRC provide an important parallel for the mechanistic details uncovered in murine studies. Our results caution against broad targeting of γδ T cells in future immune-therapy strategies, yet they also open possibilities of specific targeting of γδ T subsets based on V gene-usage or their metabolic adaptation.

Supplementary Material

Refer to Web version on PubMed Central for supplementary material.

Acknowledgements:

We thank all Mucida Lab members and Rockefeller University employees for their continuous assistance; A. Rogoz and S. Gonzalez for the maintenance of mice. We thank R. O'Brien for the anti-Vγ7 hybridoma, and Y. Belkaid for the anti-Vγ6 hybridoma. We also thank the Victora and Lafaille labs for fruitful discussions.

Funding:

National Institutes of Health grant R01CA218133 (SG)

NCTSA UL1TR001866 (YA)

The Howard Hughes Medical Institute (DM)

National Institutes of Health grant R01DK093674 (DM)

National Institutes of Health grant R01DK113375 (DM)

Food Allergy FARE/FASI Consortium (DM)

Mathers Foundation and Pershing Square Sohn Cancer Research Alliance (DM)

Black Family Metastasis Foundation (BSR)

References and Notes

1. Ettersperger J et al. , Interleukin-15-Dependent T-Cell-like Innate Intraepithelial Lymphocytes Develop in the Intestine and Transform into Lymphomas in Celiac Disease. Immunity 45, 610–625 (2016). [PubMed: 27612641]
2. Sujino T et al. , Tissue adaptation of regulatory and intraepithelial CD4(+) T cells controls gut inflammation. Science 352, 1581–1586 (2016). [PubMed: 27256884]
3. Hoytema van Konijnenburg DP et al. , Intestinal Epithelial and Intraepithelial T Cell Crosstalk Mediates a Dynamic Response to Infection. Cell 171, 783–794 e713 (2017). [PubMed: 28942917]
4. McDonald BD, Jabri B, Bendelac A, Diverse developmental pathways of intestinal intraepithelial lymphocytes. Nature reviews. Immunology 18, 514–525 (2018).
5. Edelblum KL et al. , gammadelta Intraepithelial Lymphocyte Migration Limits Transepithelial Pathogen Invasion and Systemic Disease in Mice. Gastroenterology 148, 1417–1426 (2015). [PubMed: 25747597]
6. Mikulak J et al. , NKp46-expressing human gut-resident intraepithelial Vdelta1 T cell subpopulation exhibits high antitumor activity against colorectal cancer. JCI Insight 4, (2019).
7. Scheper W, Sebestyen Z, Kuball J, Cancer Immunotherapy Using gammadeltaT Cells: Dealing with Diversity. Frontiers in immunology 5, 601 (2014). [PubMed: 25477886]
8. Silva-Santos B, Serre K, Norell H, gammadelta T cells in cancer. Nature reviews. Immunology 15, 683–691 (2015).
9. Tie G et al. , Hypercholesterolemia Increases Colorectal Cancer Incidence by Reducing Production of NKT and gammadelta T Cells from Hematopoietic Stem Cells. Cancer Res 77, 2351–2362 (2017). [PubMed: 28249902]
10. Matsuda S, Kudoh S, Katayama S, Enhanced formation of azoxymethane-induced colorectal adenocarcinoma in gammadelta T lymphocyte-deficient mice. Jpn J Cancer Res 92, 880–885 (2001). [PubMed: 11509121]
11. Wu Y et al. , An innate-like Vdelta1(+) gammadelta T cell compartment in the human breast is associated with remission in triple-negative breast cancer. Sci Transl Med 11, (2019).
12. Grivennikov S et al. , IL-6 and Stat3 are required for survival of intestinal epithelial cells and development of colitis-associated cancer. Cancer Cell 15, 103–113 (2009). [PubMed: 19185845]
13. Grivennikov SI, Greten FR, Karin M, Immunity, inflammation, and cancer. Cell 140, 883–899 (2010). [PubMed: 20303878]
14. Grivennikov SI et al. , Adenoma-linked barrier defects and microbial products drive IL-23/IL-17-mediated tumour growth. Nature 491, 254–258 (2012). [PubMed: 23034650]
15. Dmitrieva-Posocco O et al. , Cell-Type-Specific Responses to Interleukin-1 Control Microbial Invasion and Tumor-Elicited Inflammation in Colorectal Cancer. Immunity 50, 166–180 e167 (2019). [PubMed: 30650375]
16. Ma S et al. , IL-17A produced by gammadelta T cells promotes tumor growth in hepatocellular carcinoma. Cancer Res 74, 1969–1982 (2014). [PubMed: 24525743]
17. Coffelt SB et al. , IL-17-producing gammadelta T cells and neutrophils conspire to promote breast cancer metastasis. Nature 522, 345–348 (2015). [PubMed: 25822788]
18. Wu P et al. , gammadeltaT17 cells promote the accumulation and expansion of myeloid-derived suppressor cells in human colorectal cancer. Immunity 40, 785–800 (2014). [PubMed: 24816404]
19. Silva-Santos B, Mensurado S, Coffelt SB, gammadelta T cells: pleiotropic immune effectors with therapeutic potential in cancer. Nat Rev Cancer 19, 392–404 (2019). [PubMed: 31209264]

20. Fisher JP et al. , Neuroblastoma killing properties of Vdelta2 and Vdelta2-negative gammadeltaT cells following expansion by artificial antigen-presenting cells. Clin Cancer Res 20, 5720–5732 (2014). [PubMed: 24893631]
21. Tan L et al. , Single-Cell Transcriptomics Identifies the Adaptation of Scart1(+) Vgamma6(+) T Cells to Skin Residency as Activated Effector Cells. Cell Rep 27, 3657–3671 e3654 (2019). [PubMed: 31216482]
22. Okayasu I, Ohkusa T, Kajiura K, Kanno J, Sakamoto S, Promotion of colorectal neoplasia in experimental murine ulcerative colitis. Gut 39, 87–92 (1996). [PubMed: 8881816]
23. Feng Y et al. , Sox9 induction, ectopic Paneth cells, and mitotic spindle axis defects in mouse colon adenomatous epithelium arising from conditional biallelic Apc inactivation. Am J Pathol 183, 493–503 (2013). [PubMed: 23769888]
24. Hinoi T et al. , Mouse model of colonic adenoma-carcinoma progression based on somatic Apc inactivation. Cancer Res 67, 9721–9730 (2007). [PubMed: 17942902]
25. Di Marco Barros R et al. , Epithelia Use Butyrophilin-like Molecules to Shape Organ-Specific gammadelta T Cell Compartments. Cell 167, 203–218 e217 (2016). [PubMed: 27641500]
26. Jandke A et al. , Butyrophilin-like proteins display combinatorial diversity in selecting and maintaining signature intraepithelial gammadelta T cell compartments. Nature communications 11, 3769 (2020).
27. Melandri D et al. , The gammadeltaTCR combines innate immunity with adaptive immunity by utilizing spatially distinct regions for agonist selection and antigen responsiveness. Nature immunology 19, 1352–1365 (2018). [PubMed: 30420626]
28. Greten FR, Grivennikov SI, Inflammation and Cancer: Triggers, Mechanisms, and Consequences. Immunity 51, 27–41 (2019). [PubMed: 31315034]
29. Yassin M et al. , Upregulation of PD-1 follows tumour development in the AOM/DSS model of inflammation-induced colorectal cancer in mice. Immunology 158, 35–46 (2019). [PubMed: 31429085]
30. Chen Y, Chou K, Fuchs E, Havran WL, Boismenu R, Protection of the intestinal mucosa by intraepithelial gamma delta T cells. Proceedings of the National Academy of Sciences of the United States of America 99, 14338–14343 (2002). [PubMed: 12376619]
31. Lopes N et al. , Distinct metabolic programs established in the thymus control effector functions of gammadelta T cell subsets in tumor microenvironments. Nature immunology 22, 179–192 (2021). [PubMed: 33462452]
32. Ivanov II et al. , The Orphan Nuclear Receptor RORgammat Directs the Differentiation Program of Proinflammatory IL-17(+) T Helper Cells. Cell 126, 1121–1133 (2006). [PubMed: 16990136]
33. Jin C et al. , Commensal Microbiota Promote Lung Cancer Development via gammadelta T Cells. Cell 176, 998–1013 e1016 (2019). [PubMed: 30712876]
34. McAllister F et al. , Oncogenic Kras activates a hematopoietic-to-epithelial IL-17 signaling axis in preinvasive pancreatic neoplasia. Cancer Cell 25, 621–637 (2014). [PubMed: 24823639]
35. Tavazoie MF et al. , LXR/ApoE Activation Restricts Innate Immune Suppression in Cancer. Cell, (2018).
36. Rei M et al. , Murine CD27(−) Vgamma6(+) gammadelta T cells producing IL-17A promote ovarian cancer growth via mobilization of protumor small peritoneal macrophages. Proceedings of the National Academy of Sciences of the United States of America 111, E3562–3570 (2014). [PubMed: 25114209]
37. Moreau HD et al. , Signal strength regulates antigen-mediated T-cell deceleration by distinct mechanisms to promote local exploration or arrest. Proceedings of the National Academy of Sciences of the United States of America 112, 12151–12156 (2015). [PubMed: 26371316]
38. Girardi M et al. , The distinct contributions of murine T cell receptor (TCR)gammadelta+ and TCRalphabeta+ T cells to different stages of chemically induced skin cancer. JExp Med 198, 747–755 (2003). [PubMed: 12953094]
39. Cheroutre H, Lambolez F, Mucida D, The light and dark sides of intestinal intraepithelial lymphocytes. Nature reviews. Immunology 11, 445–456 (2011).
40. Mayassi T et al. , Chronic Inflammation Permanently Reshapes Tissue-Resident Immunity in Celiac Disease. Cell 176, 967–981 e919 (2019). [PubMed: 30739797]

41. Chabab G et al. , Identification of a regulatory Vdelta1 gamma delta T cell subpopulation expressing CD73 in human breast cancer. Journal of leukocyte biology 107, 1057–1067 (2020). [PubMed: 32362028]

42. Lee JS et al. , Interleukin-23-Independent IL-17 Production Regulates Intestinal Epithelial Permeability. Immunity 43, 727–738 (2015). [PubMed: 26431948]

43. Hayday AC, gammadelta T Cell Update: Adaptate Orchestrators of Immune Surveillance. Journal of immunology 203, 311–320 (2019).

44. Fahl SP et al. , Role of a selecting ligand in shaping the murine gammadelta-TCR repertoire. Proceedings of the National Academy of Sciences of the United States of America 115, 1889–1894 (2018). [PubMed: 29432160]

45. Du Y et al. , Cancer cell-expressed BTNL2 facilitates tumour immune escape via engagement with IL-17A-producing gammadelta T cells. Nature communications 13, 231 (2022).

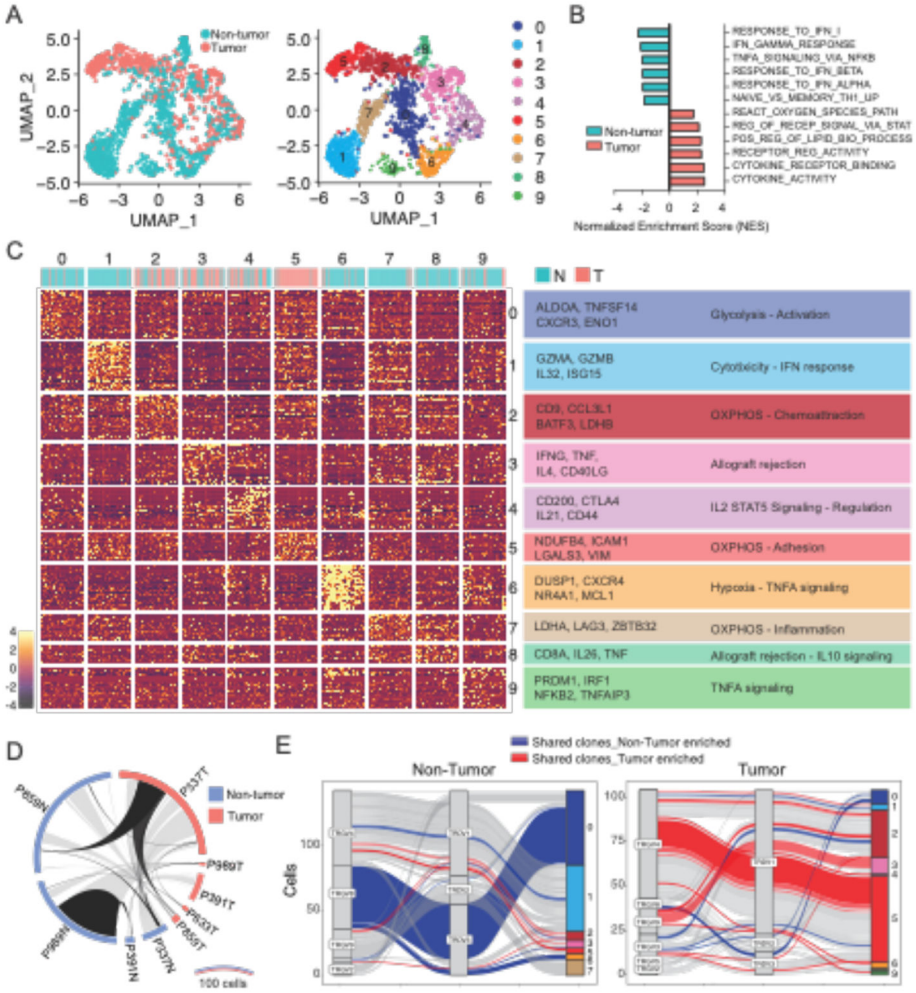

Fig. 1. Profiling of human γδ T cells in patients with CRC identifies tissue specific subsets.

(**A-E**) $\gamma\delta^+$ T cells were sorted from tumor and adjacent (non-tumor) areas of human CRC colonic resection tissue and processed for 10X Genomics RNA and TCR sequencing. Cells were stimulated with PMA/Ionomycin prior to RNA sequencing. (**A**) UMAP plot colored by tissue (left) and gene expression cluster (right) of $\gamma\delta^+$ T cells. (**B**) Gene set enrichment analysis (GSEA) of $\gamma\delta^+$ T cells recovered from non-tumor (blue) and tumor (red) areas. (**C**) Gene expression heatmap and characterization of $\gamma\delta^+$ clusters based on GSEA hallmarks. Contribution of non-tumor (blue) and tumor (red) cells in gene expression clusters is depicted above the heatmap. (**D**) Circos plot of shared clones between tissues (light gray) and between patients (black), based on amino acid CDR3 sequence. (**E**) Parallel plots depicting V gene usage and gene expression clusters of expanded clones found in non-tumor (left) and tumor (right) areas. Clones (represented by lines) shared between tissues are colored.

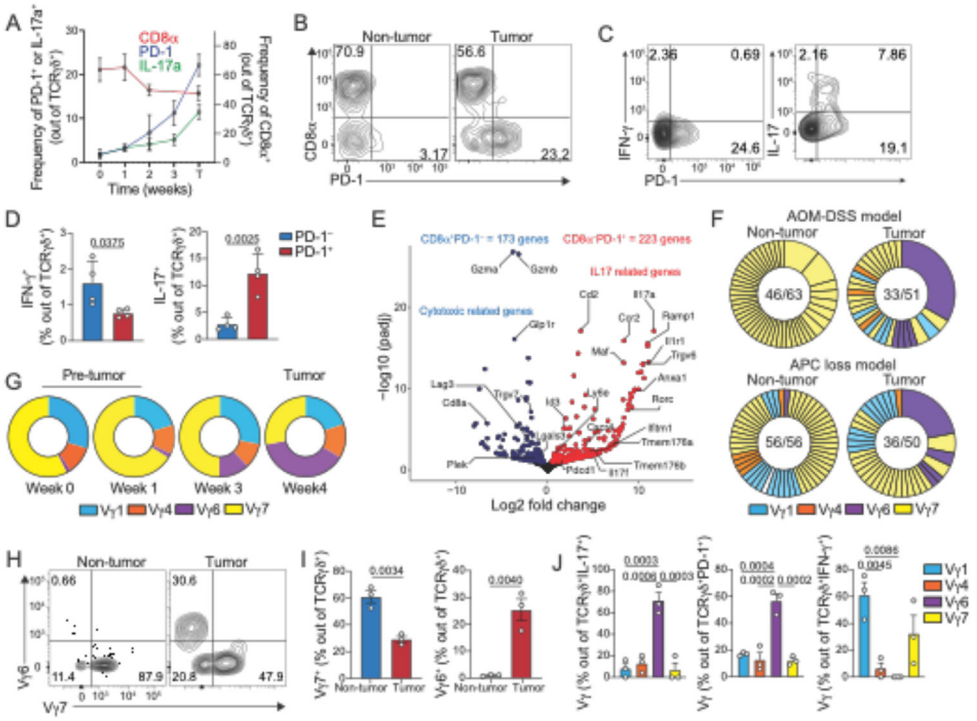

Fig. 2. Profiling tumor–infiltrating γδ T cells in CRC models reveals distinct subsets.

(**A-D**) iCdx2$^{\Delta APC}$ animals were treated with tamoxifen and sacrificed at indicated time for analysis of large intestine IEls (week 0-3) and tumor areas (T week4). (**A**) Frequency of CD8α^{+} (right axis) and PD-1^{+} or IL-17^{+} (left axis) cells among TCRγδ^{+} T cells from large intestine before (week 0) and after (week 1, 2, 3 and T) tamoxifen treatment. (**B**) Representative dot-plot of CD8α^{+} and PD-1^{+} among TCR γδ^{+} cells at 4 weeks after tamoxifen administration. (**C**) Representative dot-plot and (**D**) frequency of IFN- γ^{+} (left) or IL-17^{+} (right) among tumor-infiltrating PD-1^{+} or PD-1− TCR γδ^{+} cells (APC loss model). (**E**) Volcano plot of differentially expressed genes from RNAseq analysis of sorted CD8α^{+}PD-1$^{−}$ (blue) or CD8α$^{−}$PD-1^{+} (red) TCR γδ^{+} cells isolated from tumors of mice subjected to the AOM-DSS model. (**F**) Single-cell TCR sequencing of γδ T cells from tumor or non-tumor colonic tissue of 4 mice subjected to the AOM-DSS (top) and 4 mice from APC loss (bottom) models. Numbers in the center of pie charts represent number of clones (based on CDR3 aa sequence) per total cells sequenced. Expanded clones are fused. Clones are colored based on Vγ usage. Purple clones represent expanded Vγ6Vδ1 cell. (**G**) Pie chart of Vγ frequency among TCRγδ^{+} cells from large intestine tissue before (week 0) and after (week 1, 3 and T) tamoxifen treatment (APC loss model). (**H-J**) Vγ usage by γδ T cells from tumor or non-tumor colonic tissue of mice subjected to the AOM-DSS protocol. Representative dot-plot (**H**) and frequency (**I**) of Vγ6^{+} and Vγ7^{+} among TCRγδ^{+} cells.(**J**) Frequency of Vγ1^{+}, Vγ4^{+}, Vγ6^{+} and Vγ7^{+} among tumor-infiltrating TCRγδ^{+} cells expressing IL-17, PD-1 or IFN-γ. Representative data from 2 experiments with 3-4 animals per group. RNAseq and TCRseq data from pooled tumors. For cytokine staining, cells were stimulated with PMA and Ionomycin. Statistical P value differences are indicated. (**E, I**) two-tailed T-test, and (**J**) one-way ANOVA with Dunnett's multiple comparison test). Error bars indicate SEM.

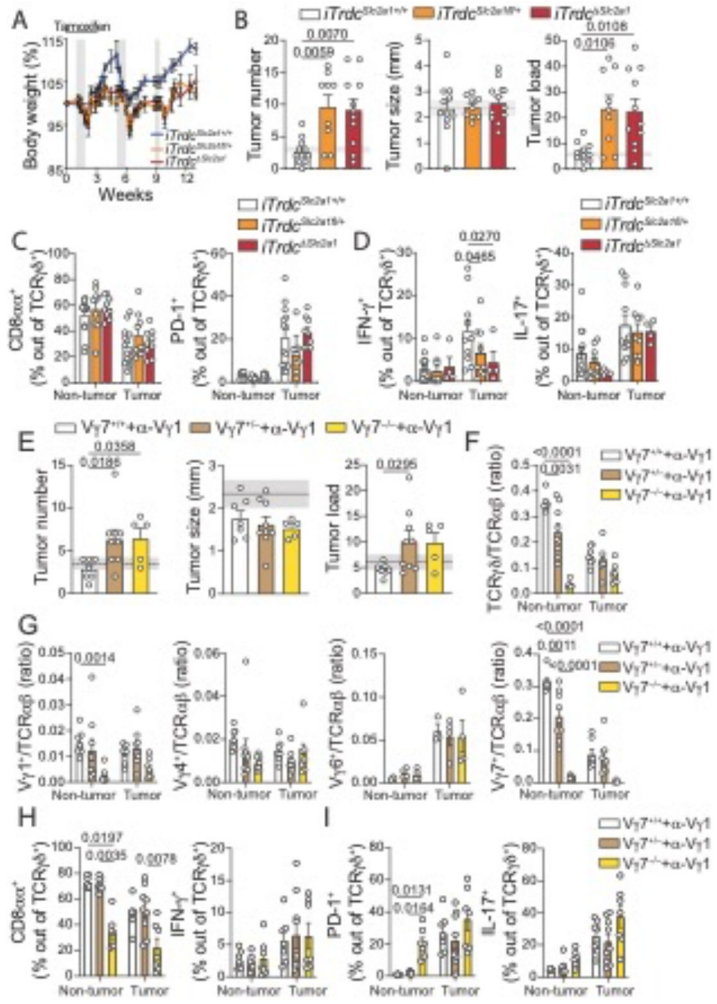

Fig. 3. Loss-of-function or depletion of epithelium-resident γδ T cells results in increased tumor numbers.

(**A-D**) *iTrdc*$^{Slc2a1fl/+}$, *iTrdc*$^{\Delta Slc2a1}$ and littermate control (*iTrdc*$^{Slc2al+/+}$) mice were subjected to AOM-DSS treatment, and tamoxifen was administered twice a week, starting 1 week before until 2 weeks after AOM injection. Animals were analyzed 12 weeks after initial AOM injection. (**A**) Mean percentage of body weight changes during AOM-DSS treatment. Gray bars represent DSS treatment. (**B**) Tumor number, size, and load. Shaded area bounded by dashed lines indicates mean ± SEM of all control C57BL6/J mice analyzed in fig. S3B (AOM-DSS model). (**C, D**) Flow cytometry analysis of γδ T cells from tumor or non-tumor colonic tissue. (**C**) Frequency of CD8α$^+$ (left) and PD-1+ (right), and (**D**) IFN-γ$^+$ (left) and IL-17$^+$ (right) among TCRγδ$^+$ cells in tumor or non-tumor colonic tissue. (**E-I**) Vγ7$^{-/-}$, Vγ7$^{+/-}$ and littermate control mice (Vγ7$^{+/+}$) were subjected to AOM-DSS model and analyzed 12 weeks after initial AOM injection. All groups were treated with 200μg of anti-Vγ1 depleting antibody (2.11) twice a week, starting one week before AOM administration until the second DSS cycle. (**E**) Tumor number, size and load. (**F**) Ratio of TCRγδ/αβ and (**G**) Vγ1/TCRαβ, Vγ4/TCRαβ, Vγ6/TCRαβ, Vγ7/TCRαβ among CD45+ cells from colonic tissue. (**H**) Frequency of CD8α$^+$ (left) and IFN-γ$^+$ (right) and (**I**) PD-1$^+$ (left) and IL-17$^+$ (right) among TCRγδ$^+$ cells. *iTrdc*$^{\Delta Slc2al}$ data are pooled from 3 experiments with

3-5 animals per group. V$\gamma 7^{-/-}$ data are pooled from 2 experiments with 3-5 animals per group. For cytokine staining, cells were stimulated with PMA and Ionomycin. Statistical P value differences are indicated. (**B-I**) One-way ANOVA with Dunnett's multiple comparison test. Error bars indicate SEM.

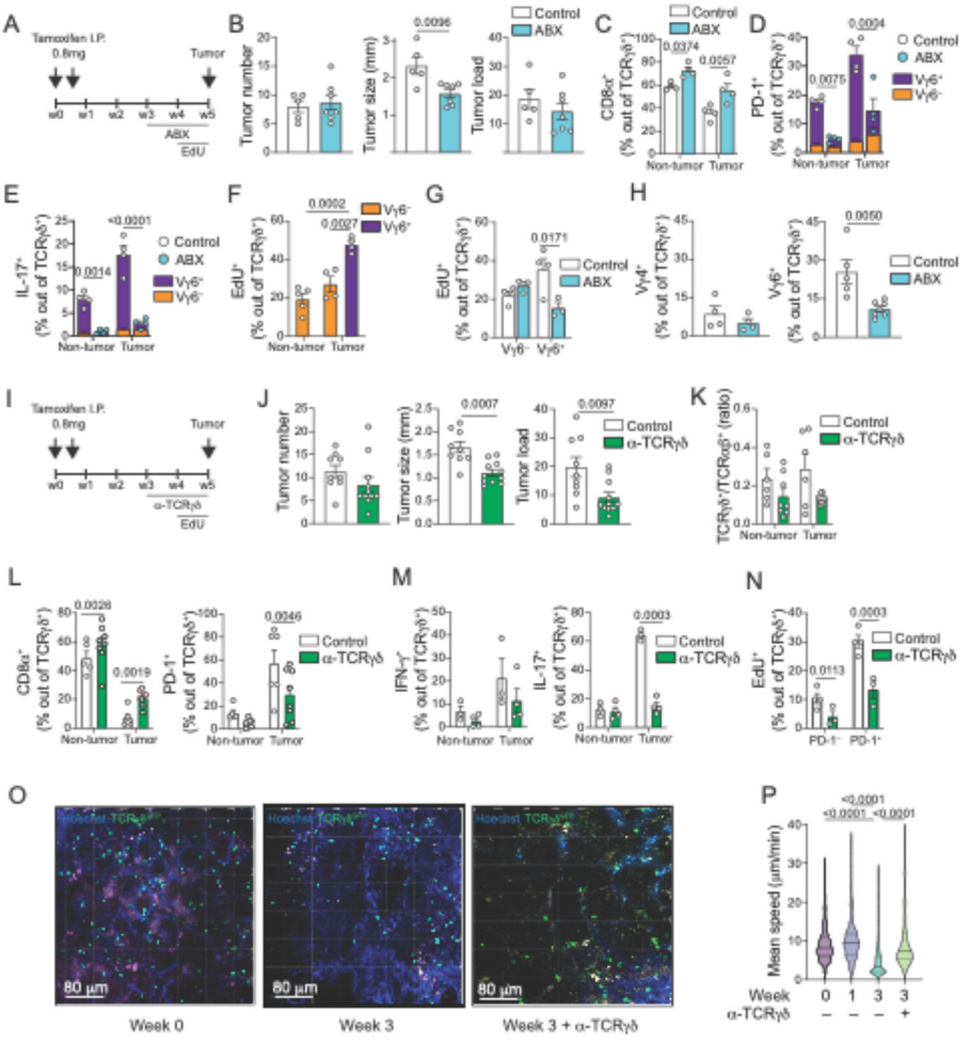

Fig. 4. Tumor-infiltrating IL~17^{+} γδ T cells induce tumor growth in a microbiota- and TCR-dependent manner.

(**A-P**) *iCdx2*$^{\Delta APC}$ mice were treated with 2 i.p. injections of 0.8mg tamoxifen and analyzed 5 weeks after (**A-N**) or at the indicated time (**O, P**). For recovery and visualization of TCRγδ^{+} cells, *iCdx2*$^{\Delta APC}$*Trdc*^{GFP} reporter mice were used (**I-P**). (**A-H**) Mice were treated with antibiotic mix (ABX) in the drinking water or (**I-N**) treated twice a week with 400μg of anti-TCRγδ blocking antibody (UC7-13D5) for the last 2 weeks of the experiment. For in vivo quantification of cell proliferation, animals were treated with EdU in the drinking water for one week before analysis. (**A, I**) Protocol. (**B, J**) Tumor number, size and load. (**C-H, K-N**) Flow cytometry analysis of γδ T cells from tumor or non-tumor colonic tissue. (**C**) Frequency of CD8α^{+} cells among TCRγδ^{+} cells. (**D**) Frequency of PD-1^{+} and (**E**) IL-17^{+} among TCRγδ^{+} cells. Vγ6^{+} (purple) vs Vγ6^{-} (orange) contribution to PD-1^{+} and IL-17–producing γδ T cells is also shown. (**F, G**) Frequency of EdU incorporation by Vγ6^{-} or Vγ6^{+} among TCRγδ^{+} cells. **G** shows tumor infiltrating cells. (**H**) Frequency of Vγ4^{+} (left) and Vγ6^{+} (right) among TCRγδ^{+} cells. (**K**) γδ^{GFP+}/TCRαβ ratio among CD45^{+} cells. (**L**) Frequency of CD8α^{+} (left) and PD-1^{+} (right), and (**M**) IFN-γ^{+} (l eft) and IL-17^{+} (right) among γδ^{GFP+} cells. (**N**) Frequency of EdU incorporation by PD-1^{-}

or PD-1^{+} among γδ^{GFP+} cells. (**O-P**) Intravital imaging of colonic γδ^{GFP+} cells. Animals were treated with α-TCRγδ blocking antibody (UC7-13D5) for 1 week before intravital imaging. (**O**) Representative image of γδ^{GFP+} cells before and 3 weeks after tamoxifen administration. Cells were tracked using *Imaris* (Bitplane AG) software. (**P**) Mean speed of individual tracks. Data from iCdx2$^{\Delta APC}$ antibiotic treated (ABX) are representative from 3 independent experiments with 3-4 animals per group. Data from iCdx2$^{\Delta APC}$ *Trdc*^{GFP} treated with UC7-13D5 are pooled from 3 independent experiments with 3-4 animals per group. Data from intravital imaging is representative of 2 experiments with 2 animals per group. (**C-G and K-N**) One-way ANOVA with Dunnett's multiple comparison test; (**B, H, J**) two-tailed t-test; (**P**) Kruskal-Wallis test with Benjamin multiple comparison test. For cytokine staining, cells were stimulated with PMA and Ionomycin. Statistical P value differences are indicated. Error bars indicate SEM.

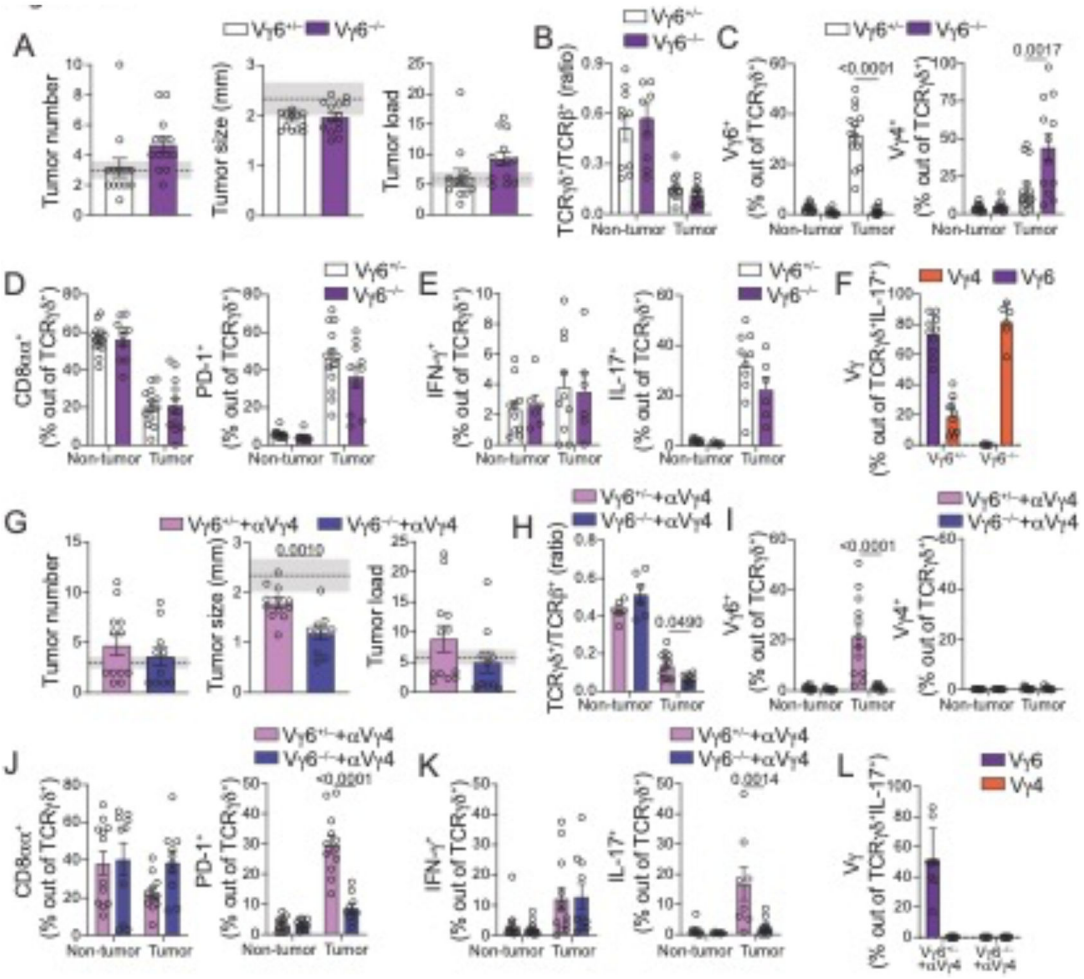

Fig. 5. Redundant tumor–infiltrating IL-17–producing Vγ6$^+$ and Vγ4$^+$ γδ cells promote tumor growth.

(**A-L**) Female Vγ6$^{-/-}$ and Vγ6$^{+/-}$ littermate control mice were subjected to the AOM-DSS protocol and analyzed 12 weeks after initial AOM injection. In panels G to L, mice received injections of 200μg α-Vγ4 depleting antibody (UC3-10A6) twice a week starting one week after the 2nd DSS cycle (last six weeks of experiment). (**A, G**) Tumor number, size, and load. Shaded area bounded by dashed lines indicates mean ± SEM of all control C57BL6/J mice analyzed in fig. S3B (AOM+DSS model). (**B-F; H-L**) Flow cytometry analysis of γδ T cells from tumor or non-tumor colonic tissue. (**B, H**) TCRγδ/αβ ratio among CD45$^+$ cells from colonic tumor tissue. (**C, I**) Frequency of Vγ6$^+$ (left) and Vγ4$^+$ (right) and (**D, J**) CD8α$^+$ (left) and PD-1$^+$ (right) among TCRγδ$^+$ cells. (**E, K**) Frequency of IFN-γ$^+$ (left) and IL-17$^+$ (right) among TCRγδ$^+$ cells. (**F, L**) Frequency of tumor-infiltrating Vγ6$^+$ and Vγ4$^+$ among IL-17–producing TCRγδ$^+$ T cells. Data from Vγ6$^{-/-}$ and α-Vγ4-treated Vγ6$^{-/-}$ are pooled from 2 and 3 experiments, respectively, with 3-6 animals per group. For cytokine staining, cells were stimulated with PMA and Ionomycin. Statistical P value differences are indicated. (**C-F; I-L**) One-way ANOVA with Dunnett's multiple comparison test; (**A, B, G, H**) two-tailed t-test. Error bars indicate SEM.